Generation of mixed triangular-rectangular meshes of arbitrary planar shapes: an algorithm for the Method of Moments

Tomasz A. Linkowski, Piotr M. Słobodzian

Wroclaw University of Technology, Wyb. Wyspianskiego 27, 50-370 Wroclaw, Poland;
e-mail: {tomasz.linkowski, piotr.slobodzian}@pwr.wroc.pl

A mesh generation algorithm for the Method of Moments (MoM) is presented here. Mesh of a shape is a set of cells (e.g. triangles) approximating this shape, and meshes are used, among others, in electromagnetic analysis with the MoM. For arbitrary planar shapes, this algorithm (named CGSM) generates a mesh comprised of mixed triangular and rectangular cells. The shape(s) to be meshed, described with line segments and arcs, may have any number of holes. Moreover, CGSM can provide non-uniform (denser) mesh near the edges of each shape. In the paper, a brief step-by-step description of CGSM is given, and then two structures are simulated using meshes created by CGSM and commercial software IE3D™.

Keywords: numerical analysis; Moment methods; mesh generation; shape.

Introduction

Mesh generation for the Method of Moments (MoM) [1] consists in approximating a shape (e.g. a polygon) with a set of non-overlapping cells (i.e. shapes like triangles, rectangles, or quadrilaterals). This process is necessary to carry out an electromagnetic analysis of this shape with the MoM.

Since the complexity of the MoM may reach $O(N^3)$ [1], where N is the number of unknowns (e.g. the number of cells), we need to minimize N. On the other hand, cells cannot be too large (i.e. N cannot be too small), as this would distort the accuracy of the analysis [2]. Therefore, CGSM approximates the shape with as many rectangles having the maximum allowed (nominal) size as possible; the remaining area is meshed with triangles.

To obtain a non-uniform mesh near edges (a.k.a. *edge meshing*), CGSM creates contours of the shape (a.k.a. *polygon offsetting* [3]) with requested width (e.g. 0.2 of the nominal length). This speeds up the MoM analysis [4]. The nominal length should equal 0.03–0.2 of the wavelength [1], and the triangles should be as close to equilateral as possible [5].

CGSM was first described in [6], and then its improved version was reported in [7]. Here, its operation is exemplified on a test shape, and meshes of a few other shapes are given.

Algorithm

The algorithm has four stages: Contour creation, Grid creation, Subdivision and Mesh generation (hence, CGSM). A test shape (Fig. 1a) will be used to demonstrate the operation of each stage.

The test shape will be meshed at 1.8 GHz, using 20 cells per wavelength and a 0.25 contour. Its overall size is 51 × 38 mm, and its vertices (`x;y`) are: `14.4;6.3|54;0.9|54;38.7| 19.8;38.7 a(3.6;18)`, **`hole`**`: 24.3;8.1 a(31.5;6.3)|36;8.1|36;18.9|24.3;18.9`, where `a(P)` is arc through `P`.

Contour creation

Several steps are taken in order to create the contours. First, each edge is translated inside (if a boundary edge) or outside (if a hole edge) by contour width (Fig. 1b).

Then, the edges are interconnected so that they form simply-connected figures (Fig. 2a). Finally, all edges are intersected, unnecessary edges are removed, and thus obtained edges are assembled into final contours (Fig. 2b).

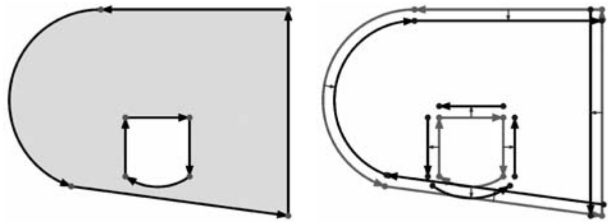

(a) (b)

Fig. 1. Contour creation: (a) test shape, (b) opposite contour edges.

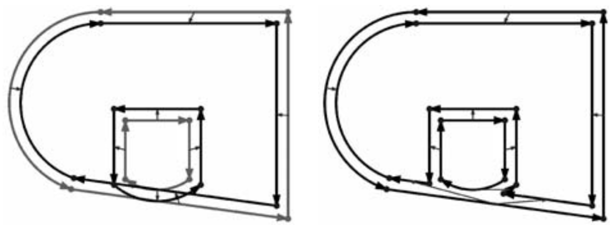

(a) (b)

Fig. 2. Contour creation: (a) interconnected edges, (b) final contours.

Grid creation

In this stage, a grid adapted to the contour edges is created. First, vertical grid lines are determined (Fig. 3a), and then the horizontal ones are added (Fig. 3b).

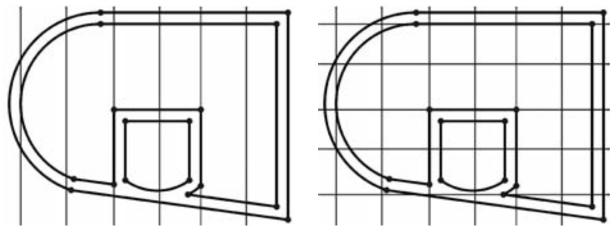

(a) (b)

Fig. 3. Grid creation: (a) vertical lines, (b) entire grid.

Subdivision of edges

Here, the edges are subdivided, i.e. cut into shorter edges. The subdivision starts with the most recently created contour and proceeds until the original shape is subdivided.

First, all edges are subdivided in grid nodes, i.e. intersections of horizontal and vertical grid lines (in our example, there are no such places). Then, horizontal and vertical segments are subdivided by vertical and horizontal grid lines, respectively (Fig. 4a). Finally, all other segments are subdivided, and all arcs are converted into segments (Fig. 4b).

For other contours, the subdivision is first based on the previously subdivided contour (so-called *descendant--based* subdivision, Fig. 5a). Then, the procedure described in the previous paragraph is applied to the remaining edges (Fig. 5b).

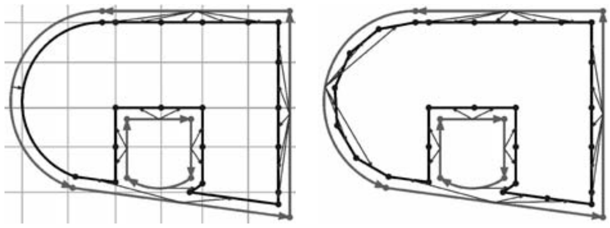

(a) (b)

Fig. 4. Subdivision: (a) horizontal and vertical segments, (b) other segments and arcs.

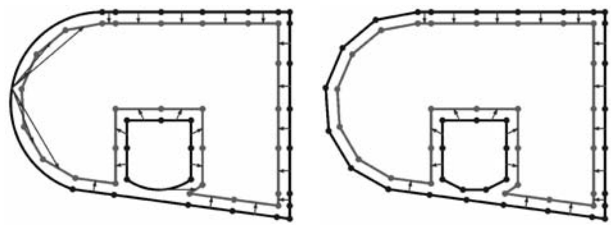

(a) (b)

Fig. 5. Subdivision: (a) descendant-based, (b) remaining edges.

Mesh generation

The final stage is the actual mesh generation. First of all, axis-aligned rectangular cells are inserted into the grid eyes wherever possible. This operation yields zero or more remaining polygons, which still need to be meshed (Fig. 6a). In order to triangulate them, they are divided into monotone polygons [8], i.e. polygons which intersect with an almost vertical line ($y=a \cdot x+b,\ a \to -\infty$) at most twice (Fig. 6b).

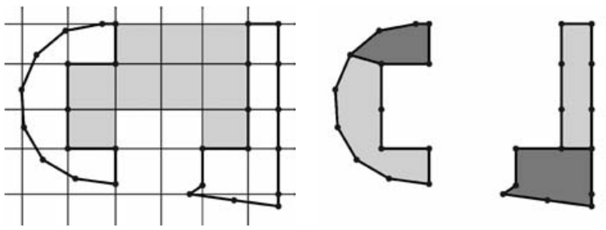

(a) (b)

Fig. 6. Mesh generation: (a) grid-based rectangles, (b) monotone remaining polygons.

These monotone polygons are then triangulated (Fig. 7a). However, such triangulation is often of poor quality, so the Delaunay flipping [8] is applied (Fig. 7b). It consists in checking whether for any pair of neighboring triangles *ABC* and *ABD*, the circumcircle of *ABC* contains vertex *D*. If so, their common edge *AB* is flipped so that we obtain triangles *ACD* and *BCD* instead. Finally, some triangles are divided in grid nodes, and some are merged into rectangles, which yields a complete interior mesh (Fig. 8a).

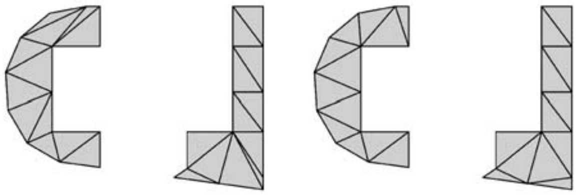

(a) (b)

Fig. 7. Mesh generation: (a) remaining polygons triangulated, (b) Delaunay flipping applied.

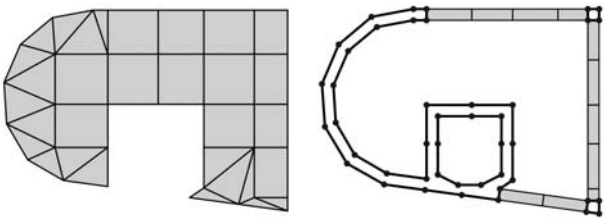

(a) (b)

Fig. 8. Mesh generation: (a) complete interior mesh, (b) descendant-based mesh.

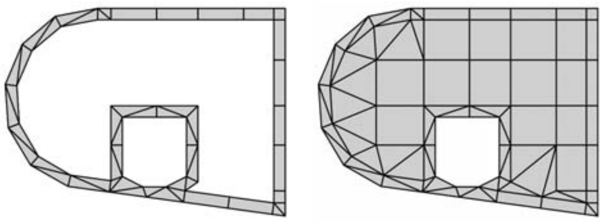

(a) (b)

Fig. 9. Mesh generation: (a) complete contour mesh, (b) final mesh (■ 25, ▲56).

For contour areas, a *descendant-based* mesh is generated first (Fig. 8b). Only afterwards, the remaining contour area is meshed like the interior (Fig. 9a). The final mesh is a sum of the interior and contour meshes (Fig. 9b).

Results

In this section, simulations of the electric current density distribution over two structures are given. Each structure is simulated using a mesh created by commercial software IE3D™ (ver. 12.35), and then using a mesh by CGSM. Always, 30 cells per wavelength are used.

The two structures are: A) a planar antenna with overall size 83 × 44 mm, and B) a "CGSM" shape with overall size 234 × 62 mm. Their meshes are given in Fig. 10 and 12, respectively. The distribution of the electric current density over their surface is presented in Fig. 11 and 13, respectively. Moreover, a summary of the results is given in Table 1.

Note that the structures are defined on a dielectric substrate with height h = 60 mil, dielectric constant ε_r = 3.4, and loss tangent $tan\ \delta$ = 0.002. Moreover, they are excited by a horizontally-polarized plane wave with inclination θ = 0, azimuth φ = 0, and magnitude: 1V.

Conclusions

In this paper, a mesh generation algorithm for the MoM that is capable of discretizing arbitrary planar

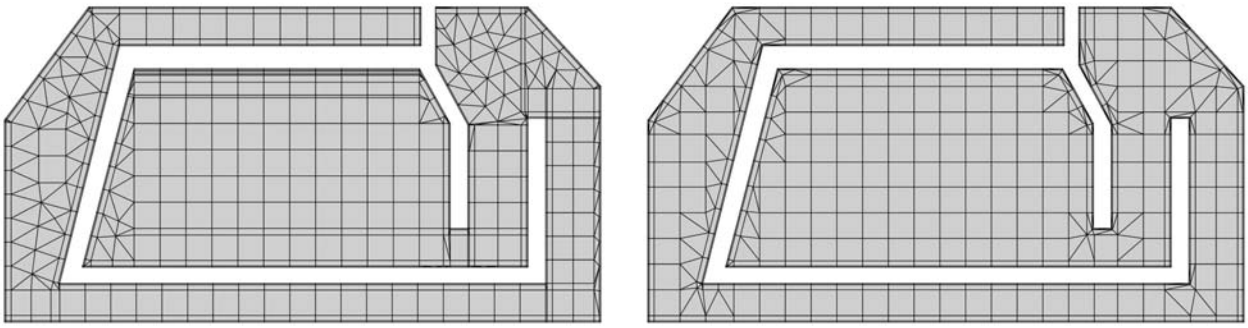

(a) (b)

Fig. 10. Planar antenna meshed at 1.8 GHz (contours: 0.05, 0.2) by: (a) IE3D™, (b) CGSM.

Table 1. Results of the MoM simulations using meshes created by IE3D™ and CGSM.

Structure	Algorithm	Cells		CC	N	t	ΔN	Δt
Planar antenna ↑	IE3D™	▲ 250	■ 604	×	1466	4.5 s	**C:** 226 (16%)	**C:** 1 s (22%)
	CGSM	▲ 232	■ 498	✓	**1240**	**3.5 s**		
"CGSM" shape ↓	IE3D™	▲ 1561	■ 783	✓	3539	25 s	**C:** 911 (26%)	**C:** 12 s (48%)
	CGSM	▲ 1204	■ 543	✓	**2628**	**13 s**		

CC — obtained correct contours, N — unknowns (internal mesh edges), t — analysis time (filling and solving of the MoM matrix), ΔN/Δt — difference in unknowns/time in favor of I (IE3D) / C (CGSM).

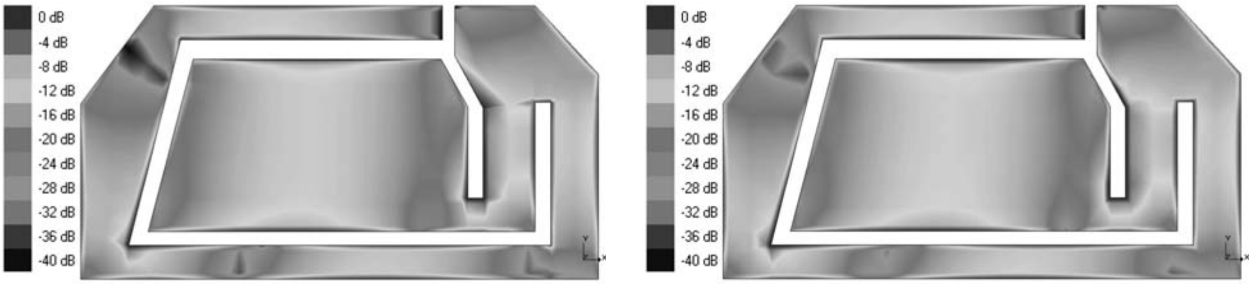

(a) (b)

Fig. 11. Electric current density (reference: 0.6 A/m) over a planar antenna (1.8 GHz) meshed by: (a) IE3D™, (b) CGSM.

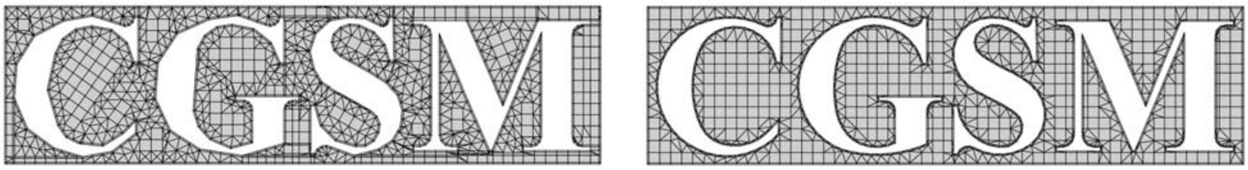

(a) (b)

Fig. 12. "CGSM" shape meshed at 1.5 GHz (contour: 0.15) by: (a) IE3D™, (b) CGSM.

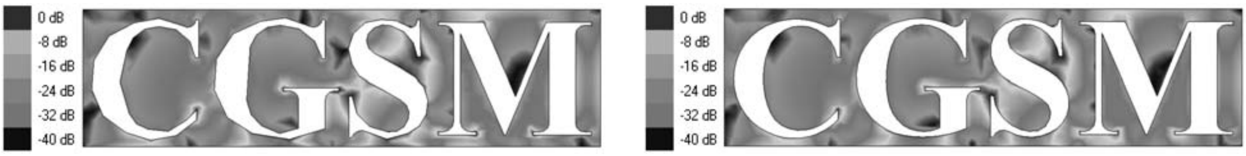

(a) (b)

Fig. 13. Electric current density (reference: 0.4 A/m) over a "CGSM" shape (1.5 GHz) meshed by: (a) IE3D™, (b) CGSM.

shapes using triangles and rectangles has been presented. This algorithm (CGSM) generates meshes with more regularly distributed and more evenly sized cells than commercial software IE3D™. As a result, the number of unknowns in the MoM is smaller, which shortens the analysis time (in our examples, by 22% and 48%).

Such performance of CGSM stems from its use of contours for providing "edge mesh," and use of an adaptive grid for uniform distribution of rectangles in the interior. As a result, it can produce regular meshes even for very complex shapes (e.g. Fig. 12b).

The distribution of current density is similar for meshes created by both algorithms. However, IE3D™ sometimes fails to provide correct "edge mesh" for some edges (e.g. top right part in Fig. 10a), which may lead to inaccuracies in the current density approximation near these places. Moreover, IE3D™ often introduces excessive triangles with very small angles (Fig. 10a, 12a), which not only unnecessarily increases the number of unknowns (and thus slows down the analysis), but also distorts the accuracy of the approximation.

References

[1] Peterson, A.F., S.L. Ray, and R. Mittra. *Computational methods for electromagnetics*. New York: IEEE Press, 1998.

[2] Newman, H., and P. Tulyathan. "A surface patch model for polygonal plates." *IEEE Trans. Antennas Propagat*. 30.7 (1982): 588–593.

[3] Held, M. *On the computational geometry of pocket machining*. Springer, 1991.

[4] Sercu, J., et al. „Full-wave space-domain analysis of open microstrip discontinuities […]." *IEEE Trans. Microw. Theory Tech*. 41.9 (1993): 1581–1588.

[5] Johnson, W.A., D.R. Wilton, and R.M. Sharpe. "Modeling scattering from and radiation by arbitrary shaped objects with the EFIE […]." *Electromagnetics*. 10.1,2 (1990): 41–63.

[6] Linkowski, T.A. *Methodology for computational domain discretization within the IE-MoM approach*, M.S. thesis. Wroclaw University of Technology, 2010.

[7] Linkowski, T.A., and P.M. Słobodzian. „Automatic mesh generation for planar structures […]." 5th European Conf. Antennas Propagat (EuCAP 2011). Rome, Italy, 2011: 1562–1566.

[8] de Berg, M., et al. *Computational geometry: algorithms and applications*. 3rd ed. Berlin: Springer, 2008.